JOURNAL OF SPACECRAFT AND ROCKETS
Vol. 38, No. 6, November–December 2001

Analytical Space Trajectories for Extremal Motion with Low-Thrust Exhaust-Modulated Propulsion

Robert H. Bishop* and Dilmurat M. Azimov†
University of Texas at Austin, Austin, Texas 78712

Optimal trajectories for spacecraft with power-limited propulsion are considered. Analytical solutions that describe motion along spiral trajectories are obtained for spacecraft with low-thrust propulsion. It is shown that the product of the specific impulse and the mass remains constant during the motion and that the spacecraft position is highly dependent on final value of the angle between thrust and local horizon. Minimization of the integral of thrust acceleration squared implies the minimization of the total transfer time. As an illustration of the solution process, the problem of transfer between elliptical orbits is analyzed.

Nomenclature

$\boldsymbol{a}$ = thrust acceleration vector
c = exhaust velocity
e = eccentricity
f = true anomaly
g = sea-level gravitational acceleration, km/s^2
I_{sp} = specific impulse, s
$\boldsymbol{l}$ = unit thrust vector
m = mass of spacecraft, kg
P = exhaust power, MW
$\bar{P}$ = maximum value of exhaust power, MW
p = semilatus rectum
$\boldsymbol{r}$ = position vector
t = flight time, s
$\boldsymbol{u}$ = control variables
$\boldsymbol{v}$ = velocity vector
$\boldsymbol{x}$ = state vector (position, velocity, mass)
β = mass flow rate, kg/s
γ = auxiliary control variable
η = auxiliary control variable
$\boldsymbol{\lambda}_r$ = vector conjugated to spacecraft's position vector
$\boldsymbol{\lambda}_v$ = primer vector conjugated to velocity vector
λ_7 = multiplier conjugated to mass
μ = gravitational parameter of central body, km^3/s^2
$\boldsymbol{\nu}$ = Lagrange multipliers
ω = argument of perigee, rad

Introduction

METHODS for constructing optimal low-thrust (LT) trajectories for spacecraft using power-limited exhaust-modulated propulsion systems is the topic of many papers; see for example Refs. 1–13. Early investigations of Melbourne and Sauer[1] and Melbourne[2] sought solutions utilizing calculus of variations approaches considering constant and variable thrust. Many research efforts considering exhaust-modulated propulsion systems are based on numerical solutions using direct or indirect approaches developed to solve boundary-value problems.[3–11] The advantage of indirect methods is that they yield a set of necessary conditions that describe a local extremum of the minimizing functional. A direct method based on differential inclusion concepts[4] was used by Coverstone-Carroll and Williams[3] to compute LT constant specific impulse trajectories for Earth–Mars and Earth–Jupiter transfers with one coast arc and for variable specific impulse Earth–Venus–Mars transfers employing unpowered gravity assist at Venus. A direct trajectory method utilized by Kluever[5] replaces the optimal control problem with a nonlinear programming problem that can be solved by sequential quadratic programming assuming that the specific impulse and thrust are constants. Minimum-time continuous thrust orbit transfer problems and minimum-time Mars capture problems have been considered by shooting, collocation methods, and nonlinear programming.[6–8] The fuel-optimal trajectories for spacecraft using variable thrust propulsion systems have been considered in the works of Chang-Diaz et al.,[9] Vadali et al.,[10] and Braden et al.[11] When numerical methods are used, the computation of optimal Earth–Mars trajectories includes the gravitational effects of the sun, Earth, and Mars. The references mentioned are obviously not a complete listing of the available papers utilizing numerical methods, but it is clear that most of the effort in recent years has been oriented toward the use of numerical optimization techniques. A much smaller group of papers appearing in the literature utilizes analytical methods employing problem-dependent approximations and simplifications. The work by Grodzovskii et al.[12] deals with the selection of optimal relations between the weight components of the spacecraft and optimal control of the propulsion system and determination of the set of optimal flight trajectories. Grodzovskii et al. showed that the variational equations may be solved by linearization of the equations of motion in the neighborhood of a certain plane Keplerian trajectory, known as the transporting trajectory, which satisfies the boundary conditions. Markopoulos[13] showed that the assumption that the thrust is tangent of the flight-path angle allows a complete analytical solution of the system of state and costate equations.

This paper is devoted mainly to the analytical investigation of optimal trajectories of a spacecraft with a LT exhaust-modulated propulsion system. It will be shown that one class of extremals can be characterized by analytical solutions of the 14th-order canonical system of equations of the variational problem. These solutions describe spiral trajectories about the center of attraction and may be used in the minimum-fuel expenditure problem of transfer between elliptical orbits. In the following sections, the underlying equations of motion and the performance functional are described. Analytical solutions are then developed for the planar motion case and applied to the problem of transfering between elliptic orbits using a spiraling trajectory. The paper concludes with a numerical example illustrating the elliptic orbit transfer solution using optimal spiraling transfers.

Problem Statement

The variational problem of determining optimal trajectories of a spacecraft moving in a central Newtonian gravity field can be formulated in the following manner. Consider the spacecraft with

Received 14 July 2000; revision received 29 May 2001; accepted for publication 5 June 2001. Copyright © 2001 by Robert H. Bishop and Dilmurat M. Azimov. Published by the American Institute of Aeronautics and Astronautics, Inc., with permission. Copies of this paper may be made for personal or internal use, on condition that the copier pay the $10.00 per-copy fee to the Copyright Clearance Center, Inc., 222 Rosewood Drive, Danvers, MA 01923; include the code 0022-4650/01 $10.00 in correspondence with the CCC.

*Professor, Department of Aerospace Engineering and Engineering Mechanics. Associate Fellow AIAA.

†Research Fellow, Department of Aerospace Engineering and Engineering Mechanics; permanent position: Associate Professor, Department of Theoretical and Applied Mechanics, Tashkent State University, 700095 Tashkent, Uzbekistan; azimov@csr.utexas.edu. Member AIAA.

mass m, the motion of which is described by the continuous vector functions position $\boldsymbol{r}$ and velocity $\boldsymbol{v}$. The spacecraft is powered by an LT, variable specific impulse propulsion system with exhaust velocity c, mass flow rate β (with maximal value $\bar{\beta}$), exhaust power $P = \beta c^2/2$ (with maximal value $\bar{P}$), and specific impulse I_{sp}, where $I_{\mathrm{sp}_{\min}} \le I_{\mathrm{sp}} \le I_{\mathrm{sp}_{\max}}$. The dynamic equations of motion can be given as[1,14]

$$\dot{\boldsymbol{x}} = \boldsymbol{f}(\boldsymbol{x}, \boldsymbol{u}) \tag{1}$$

with

$$\boldsymbol{x} = \begin{bmatrix} \boldsymbol{r} \\ \boldsymbol{v} \\ m \end{bmatrix} \qquad \boldsymbol{f}(\boldsymbol{x}, \boldsymbol{u}) = \begin{bmatrix} \boldsymbol{v} \\ -(\mu/r^3)\boldsymbol{r} + \dfrac{2P}{I_{\mathrm{sp}} g m}\boldsymbol{l} \\ -\dfrac{2P}{I_{\mathrm{sp}}^2 g^2} \end{bmatrix}$$

$$\boldsymbol{u} = \begin{bmatrix} \boldsymbol{l} \\ P \\ I_{\mathrm{sp}} \end{bmatrix}$$

where $\boldsymbol{l} = [l_1, l_2, l_3]^T$ is the piecewise continuous unit thrust vector and $\boldsymbol{u}$ is the control input vector.

The objective is to transfer the spacecraft in a fixed time from the initial state at t_0,

$$\boldsymbol{r}(t_0) = \boldsymbol{r}_0 \qquad \boldsymbol{v}(t_0) = \boldsymbol{v}_0 \qquad m(t_0) = m_0 \tag{2}$$

to the final state at t_1,

$$\boldsymbol{r}(t_1) = \boldsymbol{r}_1 \qquad \boldsymbol{v}(t_1) = \boldsymbol{v}_1 \tag{3}$$

while minimizing the performance index:

$$\mathcal{J} = \frac{1}{2}\int_{t_0}^{t_1} a^2(t)\,\mathrm{d}t \tag{4}$$

subject to the control constraints

$$h_1 := l_1^2 + l_2^2 + l_3^2 - 1 = 0, \qquad h_2 := P(\bar{P} - P) - \gamma^2 = 0$$
$$h_3 := \left(I_{\mathrm{sp}_{\max}} - I_{\mathrm{sp}}\right)\left(I_{\mathrm{sp}} - I_{\mathrm{sp}_{\min}}\right) - \eta^2 = 0 \tag{5}$$

where

$$a = c\beta/m = 2P/I_{\mathrm{sp}} g m$$

is the magnitude of the acceleration due to thrust. In this case, $\boldsymbol{u}$ is augmented to include η and γ, so that now $\boldsymbol{u} = [\boldsymbol{l}^T \; P \; I_{\mathrm{sp}} \; \eta \; \gamma]^T$.

The stationarity conditions (or Euler–Lagrange equations) may be expressed as [14]

$$\dot{\boldsymbol{\lambda}} + \left[\frac{\partial \boldsymbol{f}}{\partial \boldsymbol{x}}\right]^T \boldsymbol{\lambda} - \left[\frac{\partial \boldsymbol{h}}{\partial \boldsymbol{x}}\right]^T \boldsymbol{\nu} = 0, \qquad -\left[\frac{\partial \boldsymbol{f}}{\partial \boldsymbol{u}}\right]^T \boldsymbol{\lambda} + \left[\frac{\partial \boldsymbol{h}}{\partial \boldsymbol{u}}\right]^T \boldsymbol{\nu} = 0 \tag{6}$$

where $\boldsymbol{\nu}(\nu_1, \nu_2, \nu_3)$ are the Lagrange multipliers, $\boldsymbol{\lambda} = [\boldsymbol{\lambda}_r^T, \boldsymbol{\lambda}_v^T, \lambda_7]^T$, and the components of $\boldsymbol{h} = [h_1, h_2, h_3]^T$ are given in Eq. (5). From the conditions of stationarity of the performance index, we obtain the corner conditions

$$(\boldsymbol{\lambda})_{t_-}^* = (\boldsymbol{\lambda})_{t_+}^*, \qquad (\boldsymbol{\lambda}^T\dot{\boldsymbol{x}})_{t_-}^* = (\boldsymbol{\lambda}^T\dot{\boldsymbol{x}})_{t_+}^* \tag{7}$$

where the superscript * denotes the corner and the subscripts t_- and t_+ are immediately before and after the corner, respectively. The endpoint conditions (or transversality conditions) are[14]

$$\lambda_7(t_1) + \frac{\partial \mathcal{J}}{\partial m(t_1)} = 0, \qquad \frac{\partial \mathcal{J}}{\partial t_1} - \boldsymbol{\lambda}^T\dot{\boldsymbol{x}} = 0 \tag{8}$$

where subscript 1 denotes the final time of the flight.

The stationarity conditions given in Eq. (6) can be expressed in the following compact way:

$$\dot{\boldsymbol{\lambda}}_r = (\mu/r^3)\boldsymbol{\lambda}_v - 3(\mu/r^5)\left(\boldsymbol{\lambda}_v^T\boldsymbol{r}\right)\boldsymbol{r}, \qquad \dot{\boldsymbol{\lambda}}_v = -\boldsymbol{\lambda}_r \tag{9}$$

$$\dot{\lambda}_7 = (2P/cm^2)\boldsymbol{\lambda}_v^T\boldsymbol{l} \tag{10}$$

$$-(2/cm)\boldsymbol{\lambda}_v^T\boldsymbol{l} + (2/c^2)\lambda_7 + \nu_2(\bar{P} - 2P) = 0$$
$$(2P/c^2m)\boldsymbol{\lambda}_v^T\boldsymbol{l} - (4P/c^3)\lambda_7 + (\nu_3/g)\left(I_{\mathrm{sp}_{\max}} - 2I_{\mathrm{sp}} + I_{\mathrm{sp}_{\min}}\right) = 0$$
$$-(2P/cm)\boldsymbol{\lambda}_v + 2\nu_1\boldsymbol{l} = 0, \qquad -2\gamma\nu_2 = 0, \qquad -2\eta\nu_3 = 0 \tag{11}$$

where

$$c = I_{\mathrm{sp}} g \tag{12}$$

The third equation of Eq. (11) implies that the vector $\boldsymbol{\lambda}_v$ is parallel to the direction of thrust $\boldsymbol{l}$, that is,

$$\boldsymbol{l} = \boldsymbol{\lambda}_v/\lambda_v$$

From the Weierstrass condition, it follows that[14]

$$(P/c)\left(\boldsymbol{\lambda}_v^T\boldsymbol{l}/m - \lambda_7/c\right) \ge (\tilde{P}/\tilde{c})\left(\boldsymbol{\lambda}_v^T\tilde{\boldsymbol{l}}/m - \lambda_7/\tilde{c}\right) \tag{13}$$

where $\tilde{P}$, $\tilde{c}$, and $\tilde{\boldsymbol{l}}$ are admissible values. Suppose that $\tilde{c} = c$ and $\tilde{\boldsymbol{l}} = \boldsymbol{l}$, that is, let $\tilde{c}$ and $\tilde{\boldsymbol{l}}$ assume their optimal values. Then the switching function, denoted by χ, and given by[14]

$$\chi = \lambda_v/m - \lambda_7/c$$

is a continuous function, and from Eq. (13) it follows that

$$(\chi/c)(P - \tilde{P}) \ge 0 \tag{14}$$

Then, taking into account the continuity of $\boldsymbol{\lambda}^T\dot{\boldsymbol{x}}$ and using Eq. (14), we conclude that $P = \bar{P}$ when $\chi > 0$, $P = 0$ when $\chi < 0$, and $0 < P < \bar{P}$ when $\chi = 0$.

Depending on the specific values of γ and ν_2, it follows from Eq. (11) that the optimal trajectory may consist of arcs of three types: 1) coasting (or null thrust) arcs with $P = 0$ when $\gamma = 0$ and $\nu_2 \ne 0$, 2) maximum power arcs with $P = \bar{P}$ when $\gamma = 0$ and $\nu_2 \ne 0$, and 3) variable power arcs with $0 < P < \bar{P}$ when $\gamma \ne 0$ and $\nu_2 = 0$. In addition, depending on η and ν_3, and considering Eqs. (5) and (12), the following conditions for c may exist: 1) constant exhaust velocity with $c = c_{\max}$ or $c = c_{\min}$ when $\eta = 0$ and $\nu_3 \ne 0$ and 2) variable exhaust velocity with $c_{\min} < c < c_{\max}$ when $\eta \ne 0$ and $\nu_3 = 0$. Within the context of the given problem statement, there are many classes of trajectory optimization problems that can be considered. One class of trajectory optimization problems corresponds to variable power $0 < P < \bar{P}$ with $\gamma \ne 0$ and $\nu_2 = 0$ and constant exhaust velocity, that is, $c = c_{\min}$ or $c = c_{\max}$. Corresponding analytical solutions for this case may exist, but are not investigated here. Another important class of trajectory optimization problems corresponds to $\gamma = 0$ and $\nu_2 \ne 0$, which implies $P = 0$ or $P = \bar{P}$. In the well-known case of $P = 0$, the corresponding motion along the coasting arc may be described entirely analytically. The case of $P = \bar{P}$ with constant exhaust velocity is similar to the trajectory optimization problem using maximal thrust arcs[15] and is a different topic entirely from the one addressed here. Note that these problems are similar to the problem of motion with constant exhaust velocity ($c = \mathrm{const}$) and limited mass flow rate $0 \le \beta \le \bar{\beta}$, where $\beta = -\dot{m}$. It was shown that in the case of intermediate values of β, several classes of analytical solutions for intermediate thrust arcs exist.[16,17]

The class of trajectory optimization problem considered in this paper corresponds to the case of $P = \bar{P}$ and $c_{\min} < c < c_{\max}$. This implies that $\eta \ne 0$ and $\nu_3 = 0$. From the stationarity conditions one can deduce that

$$\lambda_v/m - 2(\lambda_7/c) = 0 \tag{15}$$

With the definition

$$b := \lambda_7 m^2 \tag{16}$$

we can utilize Eq. (15) to obtain the relationship

$$c = 2b/\lambda_v m \tag{17}$$

With the preceding expression for c, it follows that the thrust acceleration is given by

$$\boldsymbol{a} = (2\bar{P}/I_{sp}gm)\boldsymbol{l} = (2\bar{P}/I_{sp}gm)(\boldsymbol{\lambda}_v/\lambda_v) = (\bar{P}/b)\boldsymbol{\lambda}_v \tag{18}$$

It can be verified that b is an integration constant.

It can be shown that, in general, the equations of motion Eq. (1) and the stationarity conditions Eq. (6) may be rewritten in canonical form as

$$\dot{\boldsymbol{x}} = \left[\frac{\partial H}{\partial \boldsymbol{\lambda}}\right]^T, \qquad \dot{\boldsymbol{\lambda}} = -\left[\frac{\partial H}{\partial \boldsymbol{x}}\right]^T \tag{19}$$

with the Hamiltonian

$$H = \boldsymbol{f}^T\boldsymbol{\lambda} = -(\mu/r^3)\boldsymbol{\lambda}_v^T\boldsymbol{r} + \boldsymbol{\lambda}_r^T\boldsymbol{v} + (\bar{P}/2b)\lambda_v^2$$

For the case of planar motion in polar coordinate system, we have

$$\boldsymbol{r}(r;0), \qquad \boldsymbol{v}(v_1;v_2), \qquad \boldsymbol{\lambda}_v(\lambda_1;\lambda_2)$$

$$\boldsymbol{\lambda}_r[\lambda_4;\lambda_1(v_2/r) - \lambda_2(v_1/r) + \lambda_5/r]$$

Thus, Eq. (19) can be rewritten and expanded, yielding

$$\dot{v}_1 = (\bar{P}/b)\lambda_1 - \mu/r^2 + v_2^2/r, \qquad \dot{v}_2 = (\bar{P}/b)\lambda_2 - v_1v_2/r$$

$$\dot{r} = v_1, \qquad \dot{\theta} = v_2/r, \qquad \dot{m} = -(\bar{P}/2b^2)m^2\lambda_v^2 \tag{20}$$

$$\dot{\lambda}_1 = \lambda_2(v_2/r) - \lambda_4, \qquad \dot{\lambda}_2 = -2\lambda_1(v_2/r) + \lambda_2(v_1/r) - \lambda_5/r$$

$$\dot{\lambda}_4 = \lambda_1\left[v_2^2/r^2 - 2(\mu/r^3)\right] - \left(v_1v_2/r^2\right)\lambda_2 - \lambda_5\left(v_2/r^2\right)$$

$$\dot{\lambda}_5 = 0, \qquad \dot{\lambda}_7 = (\bar{P}/bm)\lambda_v^2 \tag{21}$$

where

$$H = \lambda_1\left(\frac{\bar{P}}{b}\lambda_1 - \frac{\mu}{r^2} + \frac{v_2^2}{r}\right) + \lambda_2\left(\frac{\bar{P}}{b}\lambda_2 - \frac{v_1v_2}{r}\right)$$

$$+ \lambda_4 v_1 + \lambda_5\frac{v_2}{r} - \lambda_7\frac{\bar{P}}{2b^2}m^2\lambda_v^2 \tag{22}$$

In addition to Eqs. (17) and (18), the system in Eqs. (20) and (21) has the following first integrals[12]:

$$-\frac{\mu}{r^3}\boldsymbol{\lambda}_v^T\boldsymbol{r} + \boldsymbol{\lambda}_r^T\boldsymbol{v} + \frac{\bar{P}}{2b}\lambda_v^2 = C \tag{23}$$

$$\boldsymbol{\lambda}_v^T\boldsymbol{v} - 2\boldsymbol{r}^T\boldsymbol{\lambda}_r - 5\frac{\bar{P}}{2b}\int\lambda_v^2\,\mathrm{d}t = -3Ct + C_1 \tag{24}$$

$$\lambda_5 = C_2 \tag{25}$$

where C, C_1, and C_2 are integration constants.

Computing analytical solutions to the canonical system in Eq. (19) requires one first integral. This integral is not currently known and is a matter under continuing investigation. However, there are some interesting classes of analytical solutions that can be obtained and utilized in trajectory optimization and spacecraft guidance. One such class of solutions is the topic of the remainder of this paper.

Analytical Solutions for Spiral LT Arcs

Denote the first integral in Eq. (23) for the Hamiltonian given in Eq. (22) by γ_1, that is,

$$\gamma_1 := -(\mu/r^3)\boldsymbol{\lambda}_v^T\boldsymbol{r} + \boldsymbol{\lambda}_r^T\boldsymbol{v} + (\bar{P}/2b)\lambda_v^2 = C \tag{26}$$

Similarly, denoting the first integral in Eq. (24) by γ_2, and using Eqs. (4) and (18) and the integral

$$\int\frac{a^2}{2\bar{P}}\,\mathrm{d}t = \frac{\bar{P}}{2b^2}\int\lambda_v^2\,\mathrm{d}t = \frac{1}{m} - \frac{1}{m_0}$$

we obtain

$$\gamma_2 := \boldsymbol{\lambda}_v^T\boldsymbol{v} - 2\boldsymbol{r}^T\boldsymbol{\lambda}_r - 5b/m + 5b/m_0 + 3Ct = C_1 \tag{27}$$

Using Poisson brackets for Eqs. (26) and (27), we compute

$$[\gamma_1,\gamma_2] = \left(\frac{\partial\gamma_1}{\partial\boldsymbol{\lambda}_v}\frac{\partial\gamma_2^T}{\partial\boldsymbol{v}} - \frac{\partial\gamma_1}{\partial\boldsymbol{v}}\frac{\partial\gamma_2^T}{\partial\boldsymbol{\lambda}_v}\right) + \left(\frac{\partial\gamma_1}{\partial\boldsymbol{\lambda}_r}\frac{\partial\gamma_2^T}{\partial\boldsymbol{r}} - \frac{\partial\gamma_1}{\partial\boldsymbol{r}}\frac{\partial\gamma_2^T}{\partial\boldsymbol{\lambda}_r}\right)$$

$$= 3\frac{\mu}{r^3}\boldsymbol{\lambda}_v^T\boldsymbol{r} - 3\boldsymbol{\lambda}_r^T\boldsymbol{v} + \frac{\bar{P}}{b}\lambda_v^2 = d$$

where d is a constant. Using Eq. (26) in conjunction with the Poisson bracket yields

$$\lambda_v^2 = (2b/5\bar{P})(d + 3C) = \text{const}$$

Therefore, we determine that λ_v is a constant. Note that using other first integrals yields an identical result.

Utilizing the Hamiltonian in Eq. (22) and the integral for

$$\lambda_v^2 = \lambda_1^2 + \lambda_2^2$$

coupled with its first, second, and third derivatives with respect to time yields the following invariant relations[16]:

$$\lambda_1\lambda_4 + \lambda_1\lambda_2(v_2/r) - \lambda_2^2(v_1/r) + \lambda_2\lambda_5/r = 0 \tag{28}$$

$$\lambda_4^2 + [\lambda_1(v_2/r) - \lambda_2(v_1/r) + \lambda_5/r]^2 = \lambda_v^2(\mu/r^3) - 3\lambda_1^2(\mu/r^3) \tag{29}$$

$$\left(\lambda_v^2 - 5\lambda_1^2\right)v_1 + 2v_1(\lambda_1v_1 + \lambda_2v_2) - 4\lambda_1\lambda_4 r = 0 \tag{30}$$

From the equation for the mass it follows that

$$1/m = 1/m_0 + \left(\bar{P}\lambda_v^2/2b^2\right)t \tag{31}$$

Utilizing Eqs. (25–30), we obtain the solution in terms of the angle φ between local horizon and thrust direction:

$$r^2 = -3\mu\frac{\lambda_v}{C_3}\sin^3\varphi \tag{32}$$

$$v_1 = \frac{3\sin 2\varphi}{5\sin^2\varphi - 3}s \tag{33}$$

$$v_2 = \frac{(3 - \sin^2\varphi)}{5\sin^2\varphi - 3}s \tag{34}$$

$$\lambda_4 = -\frac{\lambda_v\cos\varphi}{r}s \tag{35}$$

where

$$C_3/\lambda_v := C/\lambda_v - (\bar{P}/2)(\lambda_v/b), \qquad s := \pm\sqrt{(\mu/r)(1 - 3\sin^2\varphi)}$$

The expression for s implies the constraint that $\sin^2\varphi < \frac{1}{3}$. Hence, the denominator of Eqs. (33) and (34) is always negative. Also, Eq. (32) implies that the sign of $\sin\varphi$ and C_3 are related, such that, if $\sin\varphi < 0$, then $C_3 > 0$. Conversely, if $\sin\varphi > 0$, then $C_3 < 0$. Notice that s can be taken to be either $+$ or $-$. In practice, the sign of s selected depends on the problem statement. For example, considering Eq. (33), we find that if $\sin 2\varphi > 0$ and the range is decreasing, then necessarily $v_1 < 0$; hence, $+s$ must be used.

To obtain the solutions for the time of flight and polar angle, we use that

$$\frac{d\theta}{dt} = \frac{d\theta}{d\varphi}\frac{d\varphi}{dt} = \frac{v_2}{r}$$

to obtain the solutions as function of φ, as

$$t = \frac{1}{t_c}\left[\frac{3s\cos\varphi(1-5\sin^2\varphi)}{3-5\sin^2\varphi} - \frac{C_1}{\lambda_v}\right] \tag{36}$$

$$\theta = \frac{1}{4}\left(\frac{3}{\tan\varphi_0}+\varphi_0\right) - \frac{1}{4}\left(\frac{3}{\tan\varphi}+\varphi\right) + \theta_0 \tag{37}$$

where

$$\frac{C_1}{\lambda_v} = \frac{3\cos\varphi_0 s_0(1-5\sin^2\varphi_0)}{3-5\sin^2\varphi_0}, \qquad t_c = \frac{5}{2}\frac{\bar{P}\lambda_v}{b} - 3\frac{C_3}{\lambda_v}$$

The specific impulse I_{sp} is found from Eq. (17) to be

$$I_{sp} = 2b/g\lambda_v m \tag{38}$$

and the relationship between mass and specific impulse is given by

$$m_0/m_f = I_{sp,f}/I_{sp,0} \tag{39}$$

The independent integration constants C, λ_v, b, and φ_0 in the analytical solution depend on the initial conditions. For example, using Eq. (17) and that b and λ_v are constant, we have

$$b/\lambda_v = cm/2 = I_{sp}gm/2 = I_{sp,0}gm_0/2$$

The dependent integration constants C_1, C_3, and t_c follow from the values of the independent integration constants.

The expressions in Eqs. (32) and (37) can be used to illustrate typical spiral trajectories. Consider a departure from an initial elliptic orbit with semilatus rectum $p = 10{,}000$ km, eccentricity $e = 0.1$, $\theta_0 = 0$ rad, $\varphi_0 = 0.05$ rad, and $C_3/\lambda_v = -1.50282e{-}06$. This value of C_3/λ_v is taken from the numerical example presented in the next section. The resulting spiral LT trajectories corresponding to the final values $\varphi_1 = 0.101$, $\varphi_2 = 0.15$, $\varphi_3 = 0.25$, and $\varphi_4 = 0.35$ rad are shown in Fig. 1. As shown in Fig. 2, when the thrust angle φ is increased from φ_0 to $\varphi_f = \arcsin\sqrt{\frac{1}{3}}$, the range r increases from

$$r_0 = \sqrt{-3\mu(\lambda_v/C_3)\sin^3\varphi_0} \quad \text{to} \quad r_f = \sqrt{-3\mu(\lambda_v/C_3)\sin^3\varphi_f}$$

As shown in Fig. 3, the polar angle θ increases from θ_0 to

$$\theta_f = \tfrac{1}{4}(3/\tan\varphi_0 + \varphi_0) - \tfrac{1}{4}(3/\tan\varphi_f + \varphi_f) + \theta_0$$

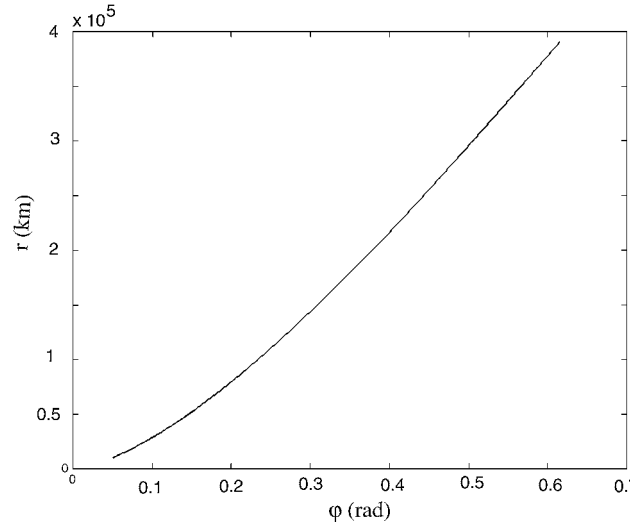

Fig. 2 Relationship between φ and r.

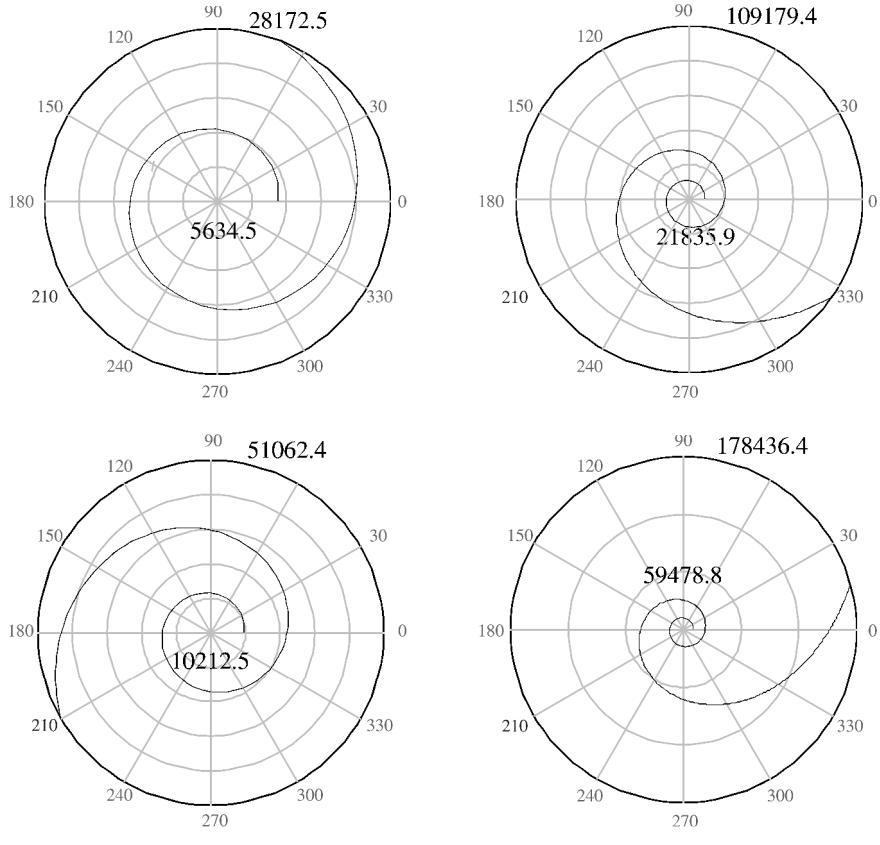

Fig. 1 LT spiral trajectories for $\theta_1 = 0$, $\varphi_1 = 0.05$, and $\varphi_2 = 0.101, 0.15, 0.25$, and 0.35.

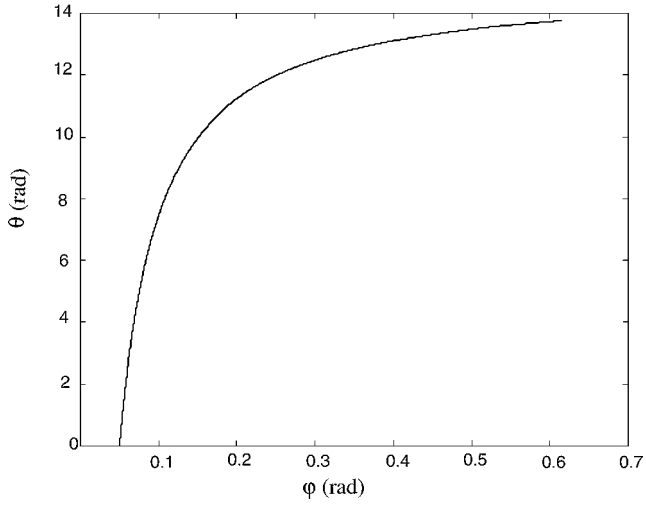

Fig. 3 Relationship between φ and θ.

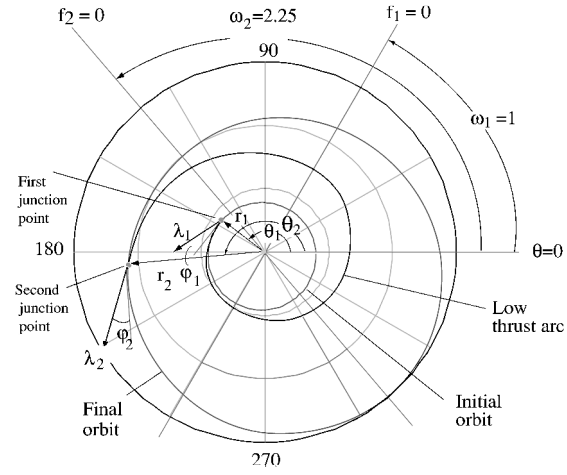

Fig. 4 Spiral LT transfer between two elliptic orbits.

As the thrust angle φ increases from φ_0 to $\varphi_f = \arcsin\sqrt{\frac{1}{3}}$, the velocity of the spacecraft decreases from

$$v_0 = \sqrt{\frac{9\sin^2 2\varphi_0 + (3-\sin^2\varphi_0)^2}{(5\sin^2\varphi_0 - 3)^2}}\sqrt{\frac{\mu}{r_0}\left(1-3\sin^2\varphi_0\right)}$$

to $v_f = 0$. The final values r_f, θ_f, and v_f correspond to an escape along a spiral trajectory that unwinds about an attracting center in the anticlockwise direction.

When the thrust angle φ is increased from $\varphi_0 = \pi - \arcsin\sqrt{\frac{1}{3}}$ (or decreased from $\pi + \arcsin\sqrt{\frac{1}{3}}$) to a specified φ_f, the range r will decrease from

$$r_0 = \sqrt{-3\mu(\lambda_v/\bar{C})\sin^3\varphi_0} \qquad \text{to} \qquad r_f = \sqrt{-3\mu(\lambda_v/\bar{C})\sin^3\varphi_f}$$

The polar angle θ will increase from θ_0 to

$$\theta_f = \tfrac{1}{4}(3/\tan\varphi_0 + \varphi_0) - \tfrac{1}{4}(3/\tan\varphi_f + \varphi_f) + \theta_0$$

and the velocity v will increase from v_0 to

$$v_f = \sqrt{\frac{9\sin^2 2\varphi_f + (3-\sin^2\varphi_f)^2}{(5\sin^2\varphi_f - 3)^2}}\sqrt{\frac{\mu}{r_0}\left(1-3\sin^2\varphi_f\right)}$$

The trajectory is a spiral which winds into the attracting center in the anticlockwise direction.

From Eqs. (33) and (34) it follows that the relationship between the flight-path angle ψ and the thrust angle φ is given by

$$\tan\psi = \frac{3\sin 2\varphi}{3-\sin^2\varphi} \tag{40}$$

Therefore, in situations where the thrust angle φ is small, we find that the tangent of the flight-path angle is approximately equal to twice the thrust angle, that is,

$$\tan\psi \approx 2\varphi \tag{41}$$

Note that Eq. (32) implies that $\sin\varphi \neq 0$; otherwise $r = 0$. As shown by Lawden[14] when considering the free final-time problem, for motion on a circular orbit, $\varphi = 0$ at any junction. Therefore, a circular orbit can not be entered into or departed from using the spiral LT arc described. In the next section, it is shown that the class of spiral LT arcs described can be used to transfer a spacecraft between elliptical orbits.

Transfer Between Elliptic Orbits

Consider the free final-time ($C = 0$) minimum-fuel transfer problem between two elliptical orbits with (p_1, e_1, ω_1) and (p_2, e_2, ω_2), respectively. In this section, we assume that the parameters of the elliptical orbit are not specified. The scenario is illustrated in Fig. 4 It is assumed that the initial and final positions of the spacecraft on the boundary elliptical orbits are not fixed and that the transfer is realized using one LT arc. This assumption implies that the trajectory being considered consists of two null thrust arcs, which are connected by one LT arc. In other words, the transfer trajectory has two junctions. The junctions are found using the continuity conditions for the state vector and primer vector. According to Eq. (7), at the junctions, the vectors $\boldsymbol{r}$, $\boldsymbol{v}$, and $\boldsymbol{\lambda}_v$ have to be continuous.[16] Therefore, using known formulas for elliptical motion and Eqs. (32–35), we obtain the following conditions of continuity at the first and second junctions:

$$(\mu/p_1)(1+e_1\cos f_1) = x_{11}\big/k^{\frac{1}{4}}, \qquad (\mu/p_1)e_1\sin f_1 = x_{21}\big/k^{\frac{1}{4}}$$

$$p_1/(1+e_1\cos f_1) = k^{\frac{1}{2}}x_{31}, \qquad \theta_1 = f_1 + \omega_1 \tag{42}$$

$$(\mu/p_2)(1+e_2\cos f_2) = x_{12}\big/k^{\frac{1}{4}}, \qquad (\mu/p_2)e_2\sin f_2 = x_{22}\big/k^{\frac{1}{4}}$$

$$p_2/(1+e_2\cos f_2) = k^{\frac{1}{2}}x_{32}$$

$$\tfrac{1}{4}(3/\tan\varphi_1 + \varphi_1) - \tfrac{1}{4}(3/\tan\varphi_2 + \varphi_2) + \theta_0 = f_2 + \omega_2 \tag{43}$$

where k is an integration constant, and

$$x_{1i} = \frac{3-z_i}{5z_i-3}d_i, \qquad x_{2i} = \frac{6\sqrt{z_i - z_i^2}}{5z_i-3}d_i, \qquad x_{3i} = \sqrt{\frac{6\mu}{\bar{P}}z_i\sqrt{z_i}}$$

$$d_i = -\sqrt{\sqrt{\frac{\bar{P}\mu}{6}}\frac{1-3z_i}{z_i\sqrt{z_i}}}, \qquad z_i = \sin^2\varphi_i \qquad (i = 1, 2)$$

From Eqs. (42) and (43), we obtain the equations

$$x_{1i}^2x_{3i}^2\left(x_{1i}^2 + x_{2i}^2\right)\big/\mu^2 - 2x_{1i}^2x_{3i}\big/\mu + 1 - e_i^2 = 0, \qquad i = 1, 2$$

which serve to find the unknowns φ_1 and φ_2. Figure 5 shows the relationship between φ and e and shows that we can transfer from an orbit with any eccentricity in the range $0 < e_1 < 1$ to any other orbit with eccentricity in the range $0 < e_2 < 1$ without violating the constraint $\sin^2\varphi < \frac{1}{3}$.

Utilizing the formulas in Eqs. (42) and (43) we obtain

$$\tan f_i = \frac{x_{1i}x_{2i}x_{3i}}{x_{1i}^2x_{3i} - \mu}, \qquad i = 1, 2$$

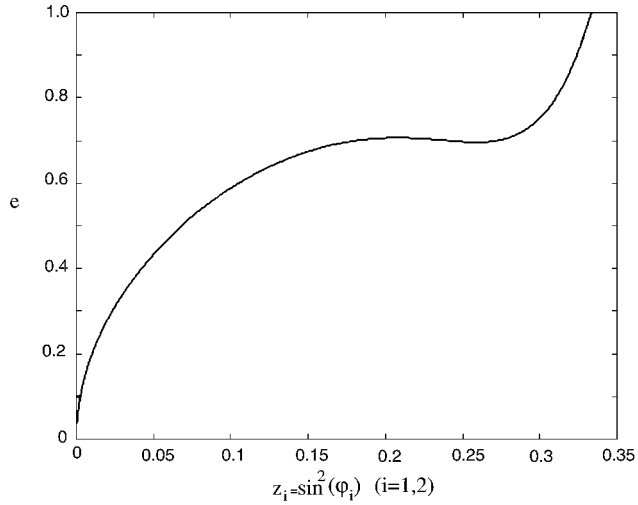

Fig. 5 Relationship between φ and the eccentricity of the transfer orbit.

from which we can find f_1 and f_2. Then,

$$\sqrt{k} = \frac{p_1 \mu}{x_{11}^2 x_{31}^2}$$

Between the semilatus recta, the following constraint must be satisfied:

$$\frac{p_1}{p_2} = \frac{x_{11}^2 x_{31}^2}{x_{12}^2 x_{32}^2} \tag{44}$$

This implies that we can specify any initial elliptic orbit with e_1 and p_1 and reach any final elliptic orbit with given e_2 but with p_2 satisfying the constraint in Eq. (44). Therefore, the value of p_2 cannot be chosen freely.

Since $k = b/\lambda_v$, the initial specific impulse can be calculated based on Eqs. (38) to be

$$I_{sp_0} = 2k/gm_0$$

The constant k and the boundary conditions given in Eqs. (2) and (3) allows us to calculate the remaining integration constants given by

$$\frac{C_1}{\lambda_v} = \frac{3d_1(1-5z_1)(1-z_1)^{\frac{1}{2}}}{k^{\frac{1}{4}}(3-5z_1)}$$

$$\frac{C_3}{\lambda_v} = -\frac{\bar{P}}{2k}$$

$$t_c = \frac{4\bar{P}}{k}$$

Consequently, the final time of the motion along the LT arc and final mass can be computed with

$$t_2 = \frac{1}{t_c}\left[\frac{3d_2(1-5z_2)(1-z_2)^{\frac{1}{2}}}{k^{\frac{1}{4}}(3-5z_2)} - \frac{C_1}{\lambda_v}\right]$$

$$\frac{1}{m_2} = \frac{1}{m_0} + \mathcal{J} = \frac{1}{m_0} + \frac{\bar{P}}{2k^2}t_2$$

To compute λ_v, we apply the transversality condition in Eq. (8), yielding

$$\lambda_{72} = -\frac{\partial \mathcal{J}}{\partial m_2} = \frac{1}{m_2^2}$$

Then from the integral in Eq. (16), we have

$$b = \lambda_{72} m_2^2 = 1$$

Therefore, from equality (38), it follows that

$$\lambda_v = 2 \big/ I_{sp_0} g m_0 = 1/k$$

The acceleration due to thrust can be determined using Eq. (18). The components of the primer vector $\boldsymbol{\lambda}_v$ in the radial and transversal directions at the first and second junctions can be computed by[14]

$$\lambda_{1i} = \lambda_v \sin\varphi_i, \qquad \lambda_{2i} = \lambda_v \cos\varphi_i, \qquad i = 1, 2$$

The continuity conditions for the primer vector are formed by equating the corresponding components on the LT arc and the terminal orbits at each junction. These equations allow us to obtain Lawden's integration constants that describe the primer vector on the initial and final orbits [14]:

$$B_i = \frac{\lambda_{1i}}{e_i \sin f_i}, \qquad D_i = [\lambda_{2i} - B_i(1 + e_i \cos f_i)](1 + e_i \cos f_i)$$

Numerical Example

Consider the free-final time ($C = 0$) minimum-fuel transfer problem between two specified elliptic orbits with parameters given as follows: initial orbit $p = 10{,}000$ km, $e = 0.1$, and $\omega = 1.0$ rad and final orbit $p = 28{,}526.2016$ km, $e = 0.2$, and $\omega = 2.25$ rad. The initial mass is $m_0 = 52{,}500$ kg and the propulsion system characteristics[10,11] are $I_{sp_{min}} = 1000$ s, $I_{sp_{max}} = 35{,}000$ s, $\bar{P} = 10$ MW with efficiency $\epsilon = 0.6$. Assuming that the spacecraft starts the transfer from the first junction at $t_1 = 0$ s, we determine that the transfer ends at the second junction after making 1.19 revolutions around the center of attraction and spending $t_2 = 223{,}627.68$ s (or $t_{2d} = 2.588$ days). The low thrust transfer characteristics are for the first junction, $r = 9991.54$ km, $\theta = 2.58$ rad, $\varphi = 0.05$ rad, $v_1 = 0.632$ km/s, $v_2 = 6.313$ km/s, $I_{sp} = 7752.04$ s, and $m = 52{,}500$ kg. For the second junction, $r = 28425.16$ km, $\theta = 10.09$ rad, $\varphi = 0.101$ rad, $v_1 = 0.75$ km/s, $v_2 = 3.738$ km/s, $I_{sp} = 7820.56$ s, and $m = 52{,}040.046$ kg. During the LT transfer, the total velocity decreases from $v_{1T} = 6.3450$ km/s to $v_{2T} = 3.8126$ km/s, while the specific impulse I_{sp} increases by 68.52 s. Using the formulas for the perfomance index and magnitude of the thrust acceleration, it can be computed that $a = 3.005 \times 10^{-6}$ km/s^2 for all t on the LT arc and $\mathcal{J} = 1.003 \times 10^{-6}$ km^2/s^3. The spacecraft uses 0.88% of the mass, while the thrust angle increases from 2.87 to 5.76 deg relative to local horizon. Utilizing the expression Eq. (40), one can observe that the flight-path angle also increases from 5.72 to 11.28 deg. In this particular maneuver, the thrust is aligned approximately in the middle between the local horizon and the velocity vector. This dependency can be seen from the time histories of these angles shown in Fig. 6. The integration constants that characterize the LT arc of the transfer trajectory, including Lawden's constants for the boundary orbits, can be easily found using the formulas given

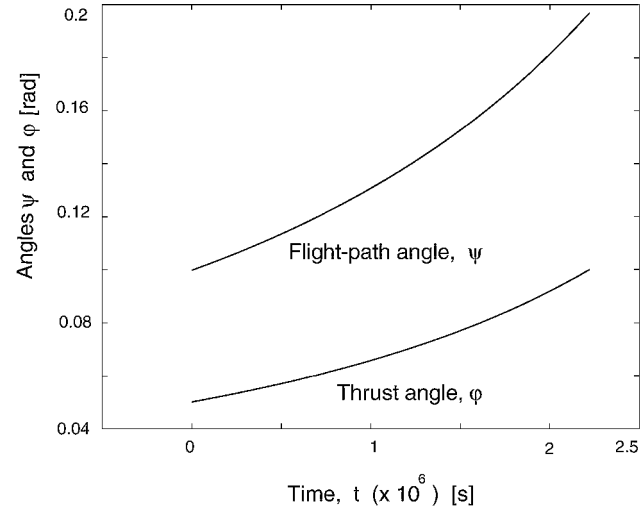

Fig. 6 Time histories of flight-path angle and thrust angle.

in the preceding section. These constants are highly sensitive to the initial conditions and can be determined only after the magnitude of the primer vector becomes known.

Conclusions

The variational problem of determining an optimal trajectory of a spacecraft equipped with a power-limited exhaust-modulated propulsion system has been considered. Analytical solutions to the problem expressed in terms of the thrust angle have been obtained using first integrals of the canonical system of equations of motion and invariant relations. These solutions describe the motion with LT along spiral trajectories around a center of attraction. It was shown that the product of the specific impulse and the mass remains constant on these trajectories and the spacecraft range is highly dependent on the thrust angle. An example of an optimal LT transfer between specified elliptical orbits was presented to illustrate the analytic solutions. As a result, from the general theory of trajectory optimization, an optimal transfer between a LT spiral arc and a circular orbit is impossible.

References

[1]Melbourne, W. G., and Sauer, C. G., Jr., "Optimum Thrust Programs for Power-Limited Propulsion Systems," *Acta Astronautica*, Vol. 8, No. 4, 1962, pp. 205–227.

[2]Melbourne, W. G., "Interplanetary Trajectories and Payload Capabilities of Advanced Propulsion Vehicles," Jet Propulsion Lab., Rept. 32-68, California Inst. of Technology, Pasadena, CA, March 1961.

[3]Coverstone-Carroll, V., and Williams, S. N., "Optimal Low-Thrust Trajectories Using Differential Inclusion Concepts," *Journal of the Astronautical Sciences*, Vol. 42, No. 4, 1994, pp. 379–393.

[4]Seywald, H., "Trajectory Optimization Based on Differential Inclusion," *Journal of Guidance, Control, and Dynamics*, Vol. 17, No. 3, 1994, pp. 480–487.

[5]Kluever, C. A., "Optimal Low-Thrust Interplanetary Trajectories by Direct Method Techniques," *Journal of the Astronautical Sciences*, Vol. 45, No. 3, 1997, pp. 247–262.

[6]Sheel, W., and Conway, B. A., "Optimization of Very-Low Thrust, Many-Revolution Spacecraft Trajectories," *Journal of Guidance, Control, and Dynamics*, Vol. 17, No. 6, 1994, pp. 1275–1282.

[7]Thorne, J. D., and Hall, C. D., "Minimum-Time Continuous Thrust Orbit Transfers," *Journal of the Astronautical Sciences*, Vol. 45, No. 4, 1997, pp. 411–432.

[8]Tang, S., and Conway, B. A., "Optimization of Low-Thrust Interplanetary Trajectories Using Collocation and Nonlinear Programming," *Journal of Guidance, Control, and Dynamics*, Vol. 18., No. 3, 1995, pp. 599–604.

[9]Chang-Diaz, F. R., Hsu, M. M., Braden, E., Johnson, I., and Yang, T. F., "Rapid Mars Transits With Exhaust Modulated Plasma Propulsion," NASA TN-3539, 1995.

[10]Vadali, S. R., Nah, R., Braden, E., and Johnson, I. L., Jr., "Fuel-Optimal Planar Interplanetary Trajectories Using Low-Thrust Exhaust -Modulated Propulsion," American Astronautical Society, AAS Paper 99-132, Feb. 1999.

[11]Braden, E. M., Cockrell, B. F., and Bordano, A. J., "Power-Limited Human Mission to Mars," Aerospace and Flight Mechanics Div., No. JSC-28436, NASA Johnson Space Center, Sept. 1998, pp. 1–35.

[12]Grodzovskii, G. L., Ivanov, Y. N., and Tokarev, V. V., "Optimization Problems in the Mechanics of Low-Thrust Space Flight," *Proceedings of the Second All-Union Conference on Theoretical and Applied Mechanics*, Israel Program for Scientific Translation, Jerusalem, 1968, pp. 201–221.

[13]Markopoulos, N., "Analytically Exact Non-Keplerian Motion for Orbital Transfers," *Proceedings of the AIAA/AAS Astrodynamics Conference*, AIAA, Washington, DC, 1994, pp. 383–412.

[14]Lawden, D. F., *Optimal Trajectories for Space Navigation*, Butterworths, London, 1963, pp. 55–99.

[15]Azimov, D. M., and Bishop, R. H., "Extremal Rocket Motion with Maximum Thrust in a Linear Central Field," *Journal of Spacecraft and Rockets*, Vol. 38, No. 5, 2001, pp. 765–776.

[16]Azimov, D. M., "A New Classes for Intermediate-Thrust Arcs of Flight Trajectories in a Newtonian Field," *Journal of Guidance, Control, and Dynamics*, Vol. 23, No. 1, 2000, pp. 142–145.

[17]Azimov, D. M., "Intermediate Thrust Arcs in Mayer's Variational Problem," *Journal of Applied Mathematics and Mechanics*, Vol. 64, No. 1, 2000, pp. 87–95.

C. A. Kluever
Associate Editor